

P&ID-based symptom detection for automated energy performance diagnosis in HVAC systems

Arie Taal,^a Laure Itard,^b

^a Department of Mechanical Engineering, The Hague University of Applied Sciences, Delft, The Netherlands

^b Research Institute OTB, Delft University of Technology, Delft, The Netherlands

Abstract

Current symptom detection methods for energy diagnosis in heating, ventilation and air conditioning (HVAC) systems are not standardised and not consistent with HVAC process and instrumentation diagrams (P&IDs) as used by engineers to design and operate these systems, leading to a very limited application of energy performance diagnosis systems in practice. This paper proposes detection methods to overcome these issues, based on the 4S3F (four types of symptom and three types of faults) framework. A set of generic symptoms divided into three categories (balance, energy performance and operational state symptoms) is discussed and related performance indicators are developed, using efficiencies, seasonal performance factors, capacities, and control and design-based operational indicators. The symptom detection method was applied successfully to the HVAC system of the building of The Hague University of Applied Sciences. Detection results on an annual, monthly and daily basis are discussed and compared.

Keywords:

Energy Performance, FDD, Symptom detection, 4S3F method, BEMS, HVAC, KPI

Abbreviations

ATES	
BEMS	Building energy management system
BMS	Building management system
DBN	Diagnostic Bayesian network
EP	Energy performance
F	Fault
FDD	Fault detection and diagnosis
HVAC	Heating, ventilation and air conditioning
KPI	Key performance indicator
OS	Operational state
P&ID	Piping & Instrumentation Diagram
S	Symptom
THUAS	The Hague University of Applied Sciences
4S3F	Four faults and three symptoms

Symbols

COP	Coefficient of performance [-]
E	Energy [kW]
EER	Energy efficiency ratio [-]
n_{tot}	Number of detections [days, hours]
n_{fault}	Number of fault detections [days, hours]
P	Power [kW]
PF	Performance factor [-]
SCOP	Seasonal coefficient of performance [-]
SEER	Seasonal energy efficiency ratio [-]
T	Temperature [°C]
Q	Heat [kJ]
W	Work [kJ]
δ	Threshold outliers during a time span [%]
ε	Deviation from expected value [%]

Indices

cond	condenser
cw	cold water
exp	expected
evap	evaporator
hp	heat pump
hw	hot water
LL	lower limit
max	maximum
mea	measured
min	minimum
mod	module
reg	regeneration
roof	roof system THUAS building

systB	ATES system (B)
systC	heat pump system (C)
systD	boiler system (D)
systG	hydronic cold water system (G)
systH	hydronic hot water system (G)
td	thermodynamic
TSA	heat exchanger
UL	upper limit

1. Introduction

Energy use in the operational phase of buildings is higher than predicted, for instance by energy simulations, during the design phase, see e.g. [1]. Continuous commissioning by a building energy management system (BEMS) can help to reduce this unnecessarily high energy consumption. However, fully automated building energy analysis systems including fault detection and diagnosis (FDD) are not often applied in practice. An important reason is that these systems are not setup and implemented simultaneously with the heating, ventilation and air conditioning (HVAC) system. In the present article, the authors develop further the symptom detection - which indicates the presence of faults - part of the 4S3F (four categories of symptoms and three categories of faults) method for energy purposes and apply it to a case study of a thermal energy generation system. The 4S3F approach using process and instrumentation diagrams (P&IDs) remains close to the way HVAC experts diagnose problems. A first draft of this method, described in [2], in which the 4S3F architecture was tested on a simple case, presented the following four types of symptoms:

- Balance based
- Energy Performance based
- Operational State based
- Additional based

Despite many studies of fault detection methods, there is still no classification of detection models with generic key performance indicators (KPIs) and associated detection rules, and the implications of detection time spans. The current article demonstrates the proposed automated symptom detection part of the 4S3F method as applied to the thermal energy plant of the THUAS (The Hague University of Applied Sciences) building in Delft, the

Netherlands, using the data in the building management system (BMS). The HVAC system that was considered has a gas boiler and a heat pump combined with an aquifer thermal energy storage (ATES) system for the storage and supply of both heat and cold. The analysis covers a whole year, thus examining the annual energy performance of the heating and cooling systems, based on 16-minute data and demonstrates the practical usability of the 4S3F architecture for an existing HVAC system.

The 4S3F diagnosis basic architecture for energy performance is briefly presented in Section 2. Section 3 presents the pre-processing part needed for energy performance diagnosis, and Section 4 studies the generic approach to symptom detection. This section is in two parts. The first describes the KPIs and the second the rules relating to these KPIs. Much attention is paid to the development of suitable generic key energy performance and operational state indicators. Section 5 describes the HVAC system considered for a case study. Sections 6 and 7 describe the implementation of the symptom detection in the case study. Section 8 evaluates the case study results, and Section 9 discusses the detection time span. Finally, Section 10 draws conclusions and recommendations concerning the implementation of the 4S3F diagnosis framework.

2. 4S3F architecture for Energy Performance Diagnosis

2.1 BMS-data based energy diagnosis

The generic structure of the processes in a BEMS consists of pre-processing, symptom detection, diagnosis and correction phases. A BEMS can be an extension of a BMS controlling an HVAC system.

In the pre-processing phase, the measurement data is prepared for the calculation of energy performance indicators. Measurement data is obtained from the BMS (or from data loggers if there is no BMS) and is usually stored in a database. Such data is susceptible to corruption due to measurement errors (e.g. sensor inaccuracy, drifting sensors) or missing data. Data correction for such instances is performed in the pre-processing phase. In addition, measurement data is not in the proper form for energy performance calculations. For example, thermal energy flows must be calculated from temperature and flow-rate sensors, missing flow rates or temperatures must be estimated using other BMS data and product specifications (resulting in soft sensor values; for soft sensors to use in HVAC systems, see e.g. [3]), and outliers must be filtered (which can be done automatically: see e.g. the BuildingEQ project [4]).

In the detection phase, symptoms of malfunctioning are detected. Faults are then diagnosed based on the observed symptoms. The last phase is the correction phase, in which it is decided which faults must be corrected, based on performance and investment considerations.

2.2 Applied 4S3F reference architecture for energy performance diagnosis

This section presents the broad outline of the 4S3F architecture (see [2] for a detailed explanation of that architecture). The automated energy performance FDD process starts with the detection of observable malfunctioning symptoms, based on the measurement points and set points in the BMS and the P&IDs which contain HVAC components and control components (actuators, sensors and controllers). These symptoms are categorised into four main types (4S), see Fig. 2.1: balance symptoms (energy, mass and pressure based), energy performance (EP) symptoms, operational state (OS) symptoms, and symptoms based on additional information, e.g. maintenance information.

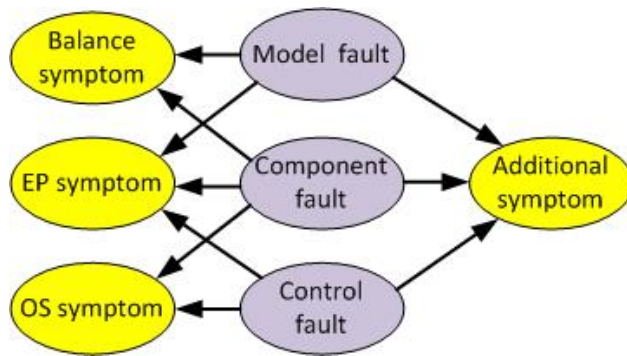


Fig. 2.1 4S3F DBN structure

The results of the symptom detection phase are supplied to a diagnostic Bayesian network (DBN) model as shown in Fig. 2.1. This model links symptoms to possible faults. We distinguish three types of faults: faults in the models used to estimate missing energy data or to set up balance models, component faults, and finally faults in control components. We define components as being not only trade components but also all HVAC subsystems at different aggregation levels. The direction of the arrows is from the faults to the symptoms. Hence Fig. 2.1 shows which symptoms may be caused by a specific fault. At fault isolation in the 4S3F method, the faults are estimated from the presence

and absence of symptoms. The components and controls, and detection rules, can be easily extracted from the HVAC P&ID. The present paper addresses only the symptom detection part (4S) of the 4S3F framework.

3. Pre-processing

On the one hand, the pre-process consists of estimating energy data automatically and continuously from the available BMS data. Missing and faulty data are corrected and calculations or assumptions for missing data points are made. This correction process can also be carried out using the 4S3F method and will be reported in another paper. In the case study for this paper all the data used had already been corrected and checked to be valid. On the other hand, an important part of the pre-process consists of the identification and selection of the systems considered for energy performance diagnosis. We propose carrying out this step once in the time interval using the HVAC P&ID and following the procedure described in Sections 4.1 and 4.2.

3.1 Selection of the systems and subsystems

For the purpose of energy performance diagnosis the HVAC system is divided into subsystems based on the availability of data that can be used to estimate relevant key performance indicators. We propose identifying three system levels for components:

- a. The whole HVAC system.
- b. Aggregated systems according to international classification agreements such as EN15316-1 [5] in which heating systems can be categorised into generator, distribution and emitter systems.
- c. Subsystems consisting of trade components (e.g. boiler and heat pump).

It is essential when choosing the aggregation levels of the various subsystems that it must be possible to measure their performance and/or make energy balances: in other words, there should be enough sensors to perform the task.

A more detailed level (e.g. components of a heat pump such as a compressor) has not been considered because we assume that FDD methods are or will be available for trade components (see [6], which presents a review of such methods for HVAC components such as chillers). The 4S3F method can of course be applied easily to trade components as well.

4. Generic approach to symptom detection

The symptom detection process determines the presence and absence of symptoms. As shown in Section 2, these can be balance, energy performance (EP) and operational state (OS) symptoms. We do not discuss the possibility of using additional information (e.g. from facility managers) as symptoms in this paper.

Like pre-processing, symptom detection is done in two stages. Firstly, all the possible symptoms are listed once in the time interval during the setup of the diagnosis system, based on the P&ID. Secondly, symptoms are detected per hour, day, week, month or year (see later in this article) using automated comparison of measured values with expected values.

Section 4.1 introduces generic symptom detection models which can be applied regardless of the HVAC system to estimate balance, EP and OS symptoms. The rules for this are elaborated in Section 4.2.

4.1 Generic symptom detection models for thermal energy plants

4.1.1 Generic energy balance symptoms

As dimensionless balance indicators we use efficiencies, in terms of heat losses in the diverse systems and components, and mechanical efficiencies. These efficiencies follow either directly from the energy balances that are made concurrently in all subsystems at various aggregation levels as shown in Section 3.1 or from efficiency rules of heat exchangers (e.g. using the NTU-method, as described in [7] or compulsory seasonal balances (e.g. for ATEs systems, see [8] which presents a review of system performance studies of such systems). If the useful energy output of a system is much lower than the

input (i.e. the efficiency is low), there is energy wasted in the system and this is a symptom that the system under consideration is not working properly. The number of systems for which efficiencies can be calculated depends of course on the measurement points present in the P&ID. Examples of formulas for these efficiencies are described in Section 7 and need to be implemented only once in the time interval.

4.1.2 Generic energy performance (EP) symptoms

A thorough literature study of possible energy performance factors was conducted. The literature includes several applications of energy performance indicators to buildings and their systems. Benchmarking approaches with simplified methods in which the energy consumptions in the buildings are compared with those of similar buildings are very common: for example, energy use intensity (EUI), which indicates energy consumption (e.g. kWh/m²) (see Chung 2011 [9] and Liu et al. [10]). However, these approaches are very rough and do not take advantage of the full potential of energy diagnostics, because they are based on the comparison of buildings and systems that are not always identical in design and use, and only aggregated seasonal or yearly data is used. Additionally, these indicators are not detailed enough to allow for the identification of HVAC-specific faults. Another approach, this time building-specific, is the use of black-box, grey-box or white-box models. Kim and Katipamula [6] presented an overview of FDD methods for HVAC systems. Wei et al. [11], Borgstein et al. [12] and Li et al. [13] presented reviews of methods for energy performance purposes. Black-box models, which are data-driven methods using e.g. ANNs (artificial neural networks) or regression models (see e.g. [14] and [15]), compare the actual energy consumptions with past performances. However, it is impossible to estimate to what extent past performances were optimal, and the setup of

a data-driven model can be time-consuming. Furthermore, the practical usability of such models is limited, because identified correlations may not be the result of causal relationships and may not have a physical meaning. Moreover, taking transient effects into account is a complex process. In grey-box models, such as RC (resistance and capacity) network models for buildings and system, the diagnosis is aided by a simple model, the parameters of which are determined by data-driven optimisation methods (see for instance ABCAT [16]). The white-box approach uses complex models based on physics (e.g. a simulation tool such as EnergyPlus, which was applied in the KnoholEM project [17]). See also Maile et al. [18], where simulation tools were proposed. These approaches are, however, also extremely time-consuming (especially the calibration procedure) and depend on the availability of reliable data for a well-functioning HVAC system. In addition, the energy performance indicators are generally not dimensionless but expressed in terms of energy intensity use, whereas in design practice dimensionless energy performance indicators such as efficiency, coefficient of performance (COP) and energy efficiency ratio (EER) are commonly used (see e.g. [14]). The main advantage is that these indicators are building-independent and reference values can be found in handbooks, guidelines and product descriptions or are known from HVAC design. We propose combining these dimensionless indicators with a few non-dimensionless indicators, related to actual energy rates of components (see e.g. DABO [19]). For instance, inadequate heat pump capacity could lead to higher energy consumption by a gas boiler at peak load, and excessive capacity could lead to higher energy consumption due to lower performance at partial load.

Finally, we noticed energy waste outliers: unexpected electrical energy consumption by fans during non-working periods, for instance. The BuildingEQ [4] project developed energy signature tools to estimate deviations between actual and expected energy values. Based on the foregoing, we propose the following classification of key (energy) performance indicators:

- Performance factors, for instance COPs and EERs. The measured COPs and EERs can be compared with product, design or guideline specifications. Mismatch can be considered as a symptom of malfunctioning.
- Capacity indicators, which can show that inadequate or excessive capacity has been installed.
- Energy outliers, which indicate energy waste.

4.1.3 Generic operational state (OS) symptoms

In addition to EP indicators, KPIs not directly related to energy amounts can be used to compare the operational performance of control components with preset values (e.g. actual temperature versus set-point temperature). DABO [19] compares actual supply water temperatures with set points. Several other studies [20 to 25] present examples of the use of energy signatures, presenting operational state values such as supply air and water temperatures in time series and scatter plots.

Based on these studies, the following operational state indicators can be considered:

- Control-based OS indicators. These check the quality of state properties against set points in the control system, for instance supply temperatures. Large numbers of wrong actual values (in comparison with the set-point value) are symptomatic of

malfunctioning. These control-based rules need to be defined in relation to the operational mode of the HVAC system (e.g. the cold well pump in the ATES system has to be on when the outlet cold well temperature is analysed).

- Design-based OS indicators. There are state values that are not controlled in the control system but that were used as a starting point for the design of the HVAC system and are expected to be achieved during operation: the supply water temperature from the cold well of the ATES system, for instance. Comparing the actual values with the design values helps to identify symptoms. The fact that design temperatures are not met could indicate that the system is not working properly, as a result of wrong HVAC design or control.

Set-point values and design values are known to the HVAC designers and generally referred to in the HVAC P&ID, in such a way that they can be listed very simply.

4.1.4 Generic additional symptoms

As well as the balance, EP and OS symptom indicators, additional information about HVAC systems can be used as symptoms, for instance:

- Maintenance information from which a component fault can be excluded.
- Result from an FDD method supplied by a component manufacturer.
- User satisfaction with thermal indoor climate.

4.2 Rules for symptom detection

In practice, measurement accuracy and precision are essential factors in the accurate determination of symptoms. Furthermore, the transient behaviour of the HVAC

components affects reliable symptom detection, and the detection time interval, e.g. hourly, daily and annual, is of great importance.

To deal with this, the detection rules need to use lower and upper limits for the threshold values. A symptom is detected when the deviation ε of an energy balance, an energy performance indicator or an operational state indicator ε is higher or lower than the threshold values ε_{min} and ε_{max} . Eq. (4.1) shows when the deviation ε is acceptable.

$$\varepsilon_{min} < \varepsilon < \varepsilon_{max} \quad (4.1)$$

Eq. (4.2) is the equation for calculating the deviation ε in the case of energy balance and EP symptom detection.

$$\varepsilon = \frac{X_{mea} - X_{exp}}{X_{exp}} \quad (4.2)$$

where:

X_{mea} = measured symptom indicator.

X_{exp} = expected symptom indicator.

The denominator X_{exp} indicates a characteristic value for the symptom indicator. The values for ε_{min} and ε_{max} depend on the type of rule and HVAC design, required control accuracy and measurement inaccuracies.

4.2.1 Rules for the detection of energy balance symptoms

The energy balance symptoms relate to dimensionless indicators (efficiencies).

For efficiencies Eq. (4.1) becomes with (4.2):

$$\varepsilon = \frac{\eta_{mea} - \eta_{exp}}{\eta_{exp}} > \varepsilon_{min} \quad (4.3)$$

For instance, ε_{\min} for efficiencies of heat distribution systems could be -5% due to measurement inaccuracies and transient behaviour. ε_{\max} is not relevant as it would indicate higher efficiencies than expected and can therefore not be considered as a symptom.

4.2.2 Rules for the detection of energy performance symptoms

Eq. (4.1) transformed for dimensionless performance factors is shown in Eq. (4.4):

$$\varepsilon = \frac{PF_{mea} - PF_{exp}}{PF_{exp}} > \varepsilon_{\min} \quad (4.4)$$

where:

PF = performance factor [-]

The dimensionless performance factors can be COPs and EERs. Acceptable deviations for COPs and EERs could be 5% ($\varepsilon_{\min} = -5\%$). Here too, ε_{\max} is not considered because a positive deviation would indicate a better COP than expected and cannot therefore be considered as faulty.

For the non-dimensionless performance factors related to capacity, a symptom is detected when the difference between the measured value P_{mea} and the nominal value P_{nom} (e.g. the installed capacity) is lower than a threshold ε_{\min} or higher than ε_{\max} . See Eq. (4.5).

$$\varepsilon_{\min} < \frac{P_{mea} - P_{nom}}{P_{nom}} < \varepsilon_{\max} \quad (4.5)$$

ε_{\min} could be -10% whereas ε_{\max} could be higher than 10%, depending on the effect of component capacity on energy performance at partial load.

For the performance factors related to energy outliers, for instance to detect unexpected energy consumption by pumps outside working hours, we propose the following equation:

$$\frac{E_{mea} - E_{exp}}{E_{exp}} < \varepsilon_{max} \quad (4.6)$$

where:

E_{mea} = measured energy consumption [J]

E_{exp} = expected energy consumption [J]

4.2.3 Rules for the detection of operational state symptoms

For operational state thresholds, we apply rules relating to the state variable under consideration. Eq. (4.7) shows the rule for temperatures:

$$\varepsilon_{min} < \Delta T < \varepsilon_{max} \quad (4.7)$$

where ΔT is the temperature deviation from the set-point or design value.

In addition, the number of faults in a time span, for instance a week, month or year, should be considered. This is because a deviation occurring only a few times will not have a large impact on energy use, whereas if it happens often the repercussions could be substantial. We propose simply using the number of faulty values n_{fault} divided by the whole number of measurements in the period under consideration. A symptom is observed when this ratio δ is larger than the threshold δ_{max} (for instance 10%). See Eq. (4.8).

$$\delta = \frac{n_{fault}}{n_{tot}} > \delta_{max} \quad (4.8)$$

δ_{\max} is estimated separately for lower (δ_{LL}) and upper (δ_{UL}) limits of the state values because negative and positive deviations may be symptoms of differing faults. The lower limit is linked to $\Delta T < \epsilon_{\min}$ and the upper limit to $\Delta T > \epsilon_{\max}$.

4.2.4 Additional conditions linked to system dynamics and time spans

Additional conditions are needed to eliminate measurement outliers and effects of transient behaviour. In addition to threshold, the dynamic of the system under consideration should be taken into account. An additional condition could be that only measurements after a certain time span are taken into account. Also, a generator's energy and temperature measurements are considered only when the generator is on.

Detection can take place at very different time intervals, from the storage interval in the BMS to annually. Using a small interval (such as the 16-minute storage interval in our case study) does not necessarily yield better symptom description, as this interval may be far below the response time of many components and would therefore necessitate the use of dynamic indicators. For instance, calculating a COP on the basis of 16-minute data makes no sense, as the COP is low at startup because the generator and hydronic systems have to be warmed up or cooled down. In the same way, the COP is very high when the generator is stopped and thermal energy is still being delivered by the hydronic systems. Conversely, aggregating the data at annual level substantially limits the possibilities for intervention, and some malfunctioning processes may not be observed. For a real-time diagnosis system, time periods of one hour, day, week or month are therefore preferable. This is discussed in Section 9. When to use which period is beyond the scope of this paper, but an automated approach in which detection at different time levels is used will

be preferable in practice. For the sake of demonstration, Section 7 presents symptom detection results in the case study on an annual basis only for balance, energy performance and operational state indicators as well as the threshold values and additional conditions used.

5. Case study: the heat and cold generation system of the building of The Hague University of Applied Sciences in Delft

The 4S3F method was tested on the THUAS building in Delft. This was selected because it has a complex HVAC system with an advanced control system, and extensive measurement data is available for analysing energy consumption and indoor climate. In addition, it is an operational HVAC system with a reputation for working properly and apparently being energy efficient.

The building mainly contains classrooms, offices for lecturers and other personnel, and a restaurant.



Fig. 5.1 Inside the THUAS building

In winter, heat is generated by a heat pump. When the heat loads are high, a gas boiler can deliver additional heat. The heat source of the heat pump is warm water delivered by the warm well of an ATES system. The ATES system can also deliver heat to the parking lane on the roof to keep it free of ice. Such ATES systems are common in the

Netherlands: more than 2,000 of them have been installed in recent years and their operation is known to be often sub-optimal.

In the summer months, cold water from the cold well of the ATES system delivers cooling. When cooling loads are high, the heat pump produces additional cold at the evaporator side. During the summer, heat from the heat pump condenser and the roof collector can be used to regenerate the warm well of the ATES system, as the annual thermal energy extracted from and pumped into the wells has to be balanced under the Dutch regulations.

As the 4S3F framework is based on HVAC P&IDs, Fig. 5.2 shows the overall principal P&ID layout with all the possible heating and cooling states of the HVAC system. The systems depicted are connected by lines which represent pipes. Each system has inlet and outlet pipes. The outlet pipes of the thermal energy plant are themselves supply pipes to the systems (34 to 38) and the inlet pipes of the energy plant are return pipes from these systems. Cold and heat are delivered to the rooms of the building by a thermal floor system which acts as a Thermally Activated Building System (TABS) and by ceiling radiation panels where water is circulated. The hot water groups (34) and (35) as well the cold water groups (36) and (37) consist of South and North groups which are divided into sub-groups (not shown) for air handling, the ceiling and the floor equipment.

Heat is produced by a heat pump (12) and a boiler (33). The heat pump extracts heat from the ATES system. Warm groundwater flows from the warm well (32) to the cold well (31) and delivers heat through a heat exchanger (8). When more heat is needed than the heat pump can deliver, the boiler provides the rest. The existing buffers (6), (10) and (16)

are needed for the stable functioning of the HVAC installation when operating under partial load.

A heat regeneration system, comprising subsystems (17) to (19), is provided to feed additional heat into the warm well of the aquifer system. Because the THUAS building needs more heat than cold, this is necessary (and mandatory) to keep both wells in thermal balance.

The hot water header (14) delivers heat to the boiler header (21), to the heat storage vessel (16) and to the regeneration unit (17). The return water is collected in the collector (15).

The main cold water header (4) delivers cold water to the header (1) and to the heat exchanger of the ground storage installation (8). The cold water header (5), which acts as a collector of warmed up return cold water from the building and the heat exchanger of the ATES system, delivers warm water to the roof (39) (so as to keep it ice-free) and to the evaporator group (11) of the heat pump (12). In the summer, the roof delivers also heat to the warm well of the ATES system.

The header (1) in the cooling group delivers cold to the building sections and Air Handling Units located with a North (N) and South (S) orientation ((36) and (37)), and also to a server room (MER) (38).

The sensors and actuators are the ones that were installed when the system was built in 2009. Fig. 5.2 shows 42 temperature sensors and 13 flow meters. There is also thermal energy metering (not shown) in the hot and cold water groups, at systems (3), (27), (28), (17), (21) and (22). Pressure metering (also not shown) is provided for the control of pumps CP28-01, CP28-02, CP29-01 and CP29-02. The electricity consumption of the

heat pump compressor (40) is measured by meter ET04-01. These measurements are stored in the BMS at 16-minute intervals. The codes of the sensors and actuators (beginning with 02 to 48) as implemented in the BMS were supplied by the designer of the HVAC system.

An entire year, 2013, was taken for the case study because of the availability of an almost complete dataset.

System and subsystem selection will be outlined in Section 6 and symptom detection in Section 7.

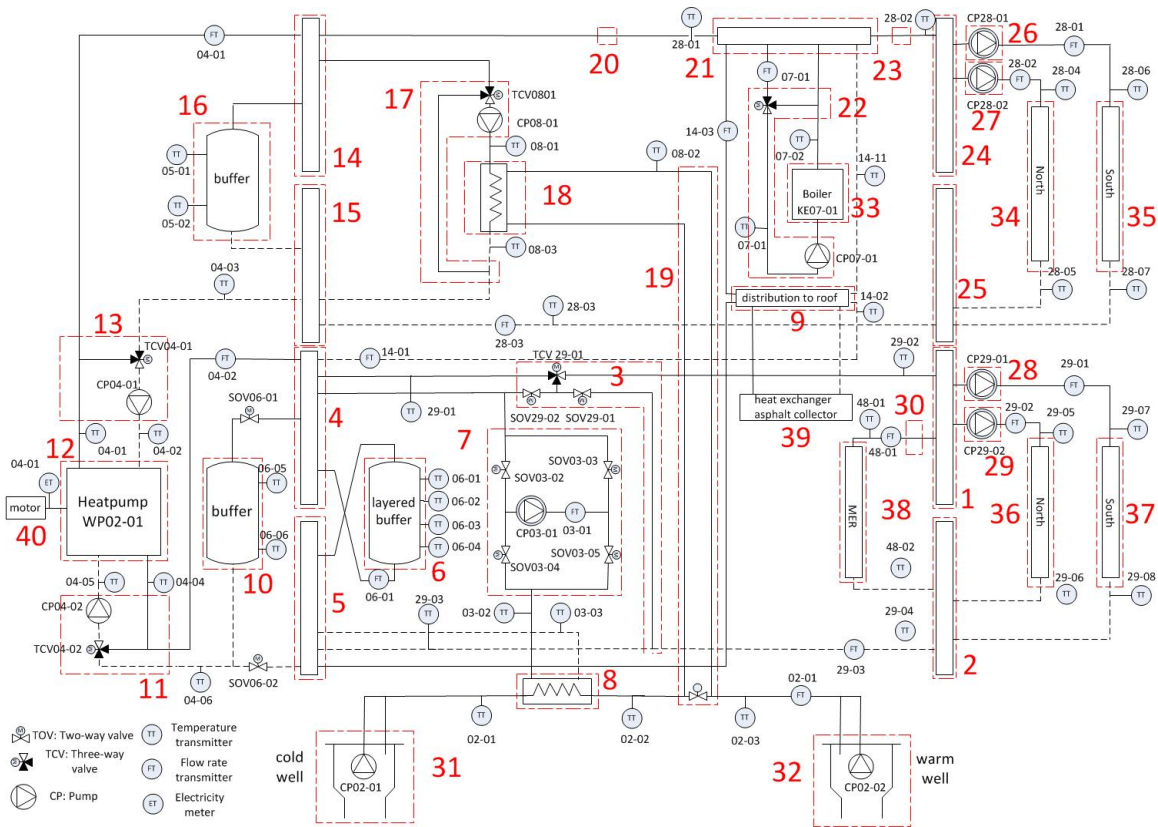


Fig. 5.2 Principal scheme (P&ID) of the heat and cold generation system of HHS (controllers are not depicted)

7. Symptom detection in the case study

This section applies the principles developed in Section 4 to the case study and shows the main detection results. We refer to the tables in Appendix A, which provide more detailed information on the detection process.

For the sake of simplicity, a detection period of one year has been taken. We consider shorter detection periods in Section 9. First, we address the balance symptoms (Section 7.1), then the energy performance symptoms (Section 7.2), and finally the operational state symptoms (Section 7.3). Section 7.4 discusses the symptoms present and absent in the case study.

7.1 Energy balance symptoms in the case study

The energy balance indicators (efficiencies (η)) specific to the HVAC system of THUAS are presented below.

For the once-in-the-time-interval implementation in the BEMS to calculate the efficiencies, the heat transfer ΔQ between systems was calculated using Eq. (7.1) for each 16 minutes, based on the flow rates and temperatures at the start time of each 16-minute interval.

$$\Delta Q = q_V \cdot \rho \cdot c \cdot \Delta T \cdot \Delta t \quad (7.1)$$

where:

ΔQ = exchanged heat [kJ]

Δt = $t_{\text{end}} - t_{\text{start}} = 960$ s.

t_{end} = end-time calculation stored in BMS [s]

t_{start} = start-time calculation stored in BMS [s]

q_v = water flow rate at start time [m³/s]

ρ = water density = 1000 kg/m³

c =specific heat of water = 4.18 kJ/kgK

ΔT = difference between supply and return temperatures at start time [K]

Eq. (7.1) can easily be programmed once in the BMS or in a separate BEMS when setting up the diagnosis system based on the P&ID. The efficiencies of the systems during a certain period are then calculated based on these ΔQ s. For instance, the efficiency of system H (see Fig. 6.1 which shows the annual exchanged energy values) is calculated using:

$$\eta_H = \frac{Q_{hw} + Q_{reg}}{Q_{cond_mod} + Q_{boiler_mod} + Q_{roof_hw}} \quad (7.2)$$

We assume an expected efficiency of $\eta_{exp} = 98\%$ (i.e. 2% heat losses) for all thermal energy balances, and a symptom when the arbitrary threshold $\epsilon_{min} = -3\%$ is exceeded. This means that when using Eq. (4.3), a symptom is detected when the efficiency is lower than 95%. One exception is made for the ATES system. The expected efficiency η_{exp} is set to 96% because of dissipation by the ATES pumps and higher thermal energy losses underground, which leads to symptom detection when the efficiency is lower than 93%. In addition to these efficiencies based on the application of system theory to the HVAC P&ID, efficiencies relating to heat exchange performance can be defined.

Eq. (7.3) is the equation for the annual efficiency of the heat balance of the ATES system (depicted in Fig. 6.1) which under the Dutch regulations needs to be 100%. Please note that η_{reg} , which is discussed in [26], can only be used in the case of annual analysis.

$$\eta_{reg} = 1 - \frac{abs(Q_{load} - Q_{unload})}{max(Q_{load}, Q_{unload})} \quad (7.3)$$

Eq. (7.4) shows the annual efficiency of the heat exchanger of the ATEs system (see Fig. 6.1 and system 8 in Fig. 5.2, which shows the heat exchanger (8) and sensors TT02-01, TT02-02 and TT03-03), based on temperature efficiency instead of the NTU method (this is an arbitrary choice).

$$\eta_{TSA} = \frac{Q_{\text{unload}}}{Q_{\text{unload,max}}} = \frac{\sum(TT02_01-TT02_02)}{\sum(TT02_01-TT03_03)} \quad (7.4)$$

According to the design, this efficiency should be at least 87%. It is assumed that a deviation threshold of 5% is acceptable.

7.2 Energy performance symptoms in the case study

This section presents the equations used to estimate the EP factors for performance factors, capacities and energy outliers.

7.2.1 Performance factors

Eqs. (7.5) to (7.7) show the performance factors for the aggregated systems under consideration: the hot water system E, the cold water system A and the roof system F. SCOP_{hw} is the seasonal COP for the heat supply to the hot water system E. SEER_{cw} (Seasonal energy efficiency ratio cold water) defines the ratio between the cold supply to the cold water system A and the energy consumption of the heat pump and the pumps in cooling mode. SCOP_{roof} denotes the SCOP for the roof heating. See Fig. 6.1, which shows the energy amounts.

$$SCOP_{hw} = \frac{Q_{hw}}{W_{hp}+W_{02}+W_{03}+W_{04}+W_{07}+Q_{gas}} \quad (7.5)$$

$$SEER_{cw} = \frac{Q_{cw}}{W_{hp}+W_{02}+W_{03}+W_{04}} \quad (7.6)$$

$$SCOP_{Proof} = \frac{Q_{roof_cw}}{W_{14}+W_{02}+W_{03}} \quad (7.7)$$

W14 is the work of the pumps in the roof collector group (not shown in Fig. 5.2 or Fig. 6.1). It only includes Whp, W02, W03, W04, W07 and W14 by the heat pump and the pumps needed for the thermal energy Q under consideration.

Eqs. (7.8) and (7.9) show the SCOP and SEER for the heat pump.

$$SCOP_{hp} = \frac{Q_{cond_mod}}{W_{hp}} \quad (7.8)$$

$$SEER_{hp}^1 = \frac{Q_{evap_mod}}{W_{hp}} \quad (7.9)$$

Eq. (7.10) defines the SCOP for heat regeneration. SCOPreg can be considered as a generic energy performance factor for ATEs systems. W14, W08 and W02 are the pump energy for heat regeneration purposes.

$$SCOP_{reg} = \frac{Q_{reg}}{W_{14}+W_{08}+W_{02}} \quad (7.10)$$

When the heat pump is simultaneously generating cold and heat for the emitter systems A, E and F, the electricity is divided proportionally based on the thermal energy supplied to systems A, E and F.

In this paper, we assume that a symptom is present when the measured SCOP or SEER is 5% lower than the expected value. International references for performance factors are not available, as the ATEs system in the THUAS building is typical for the Netherlands.

For the expected value, such as PF_{exp} in Eq. (4.4), we therefore use the Dutch guideline

¹ Here we define SEER as the seasonal quotient of heat supplied to the evaporator of the heat pump and the work supplied when the heat pump functions simultaneously in both heat and cold production mode.

ISSO 39 [27], which describes thermal energy generation plants with ATEs systems.

These expected values can be found in Table A.2.

7.2.2 Capacities

The actual capacities can be determined by identifying the maximum heat flows P occurring during the measurement period. These values are compared with the nominal power of the apparatus and the heat and cold demand (see Table A.2). A threshold of $\varepsilon_{\min} = -10\%$ is applied. Positive deviations would show that the system is working better than expected and are not therefore considered as symptoms.

7.3 Operational state symptoms in the case study

The approach using OS rules is also generic and can be set up once, for instance using a guideline. In most cases the thresholds are specific and need to be programmed only once in the particular BEMS, although default values can be used as well. Only design values of the temperature type are used in this paper. It goes without saying that far more rules than shown in this paper can be implemented: for instance, concerning pump flows and the heat shares delivered by the heat pump and boiler, or the cold delivered by the ATEs system and the heat pump, or comparisons between design water flow values and measured values. We have omitted this from the present paper for the sake of simplicity. Control-based rules are described first with the results of the detection process, followed by design-based rules for the year considered. As an additional condition, the measured values are considered if the system under consideration is operating for at least 30 minutes.

The detection period is a full year. For every day the mean weighted measured operational state value is calculated using the 16-minute values. If there are no measured values, that day is ignored. Thus we have at most $n_{\text{tot}}=365$ in the detection period under consideration in Eq. (4.8).

7.3.1 Control-based rules

In the case study we consider the control set points of the systems' inlet and outlet temperatures. The supply water temperature of the hot and cold water emitter systems E (Thw_supply) and A (Tcw_supply) is set by the control system. In addition, the outlet temperatures of the water to the evaporator (Tevap_out) and condenser (Tcond_out) from the heat pump have specific set-point values. The inlet water temperatures to the cold and warm wells of the ATES system (Tcold_well_in and Twarm_well_in) are also controlled. In the case study the average daily deviation $\varepsilon=\Delta T$, as shown in Eq. (4.7), is calculated to estimate OS symptoms. When the additional conditions mentioned in Section 4.2.4 are met, the value 1 is added to the counter n_{tot} in Eq. (4.8) for the whole year. In addition, a detected symptom is counted as 1, otherwise as 0, and added to the annual fault counter n_{fault} in Eq. (4.8).

For the supply temperatures in the hot water circuit the assumed threshold ε_{max} is 3 K, due to control accuracy and transient behaviour. However, the control of the cold water has to be more accurate, as these values greatly affect the performance of the ATES system. Accurate cold water controls are therefore provided, with three-way valves as actuators. An arbitrary threshold of 1 K is thus taken into account.

The inlet temperatures to the warm and cold wells of the ATES are essential and therefore controlled strictly, yielding an assumed threshold of 1 K.

Table A.3 shows the controlled values, which are derived from the design specification of the HVAC system of the THUAS building as shown in the HVAC P&ID.

7.3.2 Design-based rules

For the design-based rules we consider the water temperatures of systems A, B, C and E, for which either the inlet or outlet design temperatures are known. These temperatures are not controlled. We assume the same thresholds that have been applied to the control-based temperatures, i.e. 3 K at the warm water side and 1 K at the cold water side.

Table A.4 does not show the lower limit δ_{LL} and the upper limit δ_{UL} everywhere: where they are absent, the threshold can be ignored because negative and positive deviations have different meanings. For instance, if T_{hw_return} is too low it will not decrease the COP of the heat pump, whereas it will if it is too high. In the same way a higher $T_{warm_well_out}$ and T_{evap_in} are favourable. And a high T_{cw_return} helps to feed high-temperature heat into the warm well of the ATES system. Finally, a low $T_{cold_well_out}$ is desirable to avoid additional cooling by the heat pump. These rules are generally known by HVAC designers.

7.4 Symptoms detected in the case study

Appendix A shows results from the symptom detection process, which are discussed below.

Results from energy balances

Table A.1 shows the results for energy balance symptoms. Rules for the efficiencies η of the systems B to D and G and H do not generate symptoms, because all the annual deviations remain higher than ε_{\min} during the year under consideration. The heat exchanger TSA of the ATES system also shows no symptoms, but the efficiency η_{reg} is far below the expected value, showing that the ATES system is unbalanced.

Results from energy performances

The results and reference values for the detection of EP symptoms are shown for the year 2013 in Table A.2. Most of the EP indicators are true, even better than the reference values, indicating high performance. For the SCOPs and SEERs, no symptoms are detected, except for SCOP_{Proof}, which is more than 5% lower than the expected value. In terms of capacity, most of the measured values are almost the same as the designed values. However, the maximum heat transfer power produced by the heat exchanger of the ATES system is much lower than the designed value and a symptom is therefore found. The capacity of the cold water system A is also lower than designed and a symptom is detected here too. Symptoms of energy outliers were not found and are not therefore reported in Table A.2.

Only three EP factors are false and should be considered as symptoms: SCOP_{Proof}, P_{cw} and PTSA.

Results from operational states

The detection process (see Table A.3) reveals a symptom of malfunctioning for four operational states: for the supply temperatures of the hot water system E, the cold water system A and the inlet temperatures of the cold water well and warm water well. Table

A.4 summarises the design-based rules for detection purposes and the results of the detection process. One symptom is detected: the outlet temperature from the warm well.

Overview of the symptoms detected

Table 7.1 summarises the results of the annual detection process.

Table 7.1 Overview of the detection results (**P**= symptom detected, **A** symptom absent)

Energy balance symptoms		Energy performance symptoms				Operational state symptoms			
Efficiency	A/ P	Performance factor	A/ P	Capacity	A/ P	Control-based	A/ P	Design-based	A/ P
$\eta_{\text{sys}tB}$	A	SCOP _{hw}	A	Phw	A	Thw_supply	P	Thw_return	A
$\eta_{\text{sys}tC}$	A	SEER _{cw}	A	Pcw	P	Tcw_supply	P	Tcw_return	A
$\eta_{\text{sys}tD}$	A	SCOP _{proof}	P	Php	A	Tcond_out	A	Tevap_in	A
$\eta_{\text{sys}tG}$	A	SCOP _{preg}	A	Proof	A	Tevap_out	A	Tcold_well_out	A
$\eta_{\text{sys}tH}$	A	SCOP _{hp}	A	Preg	A	Tcold_well_in	P	Twarm_well_out	P
η_{TSA}	A	SEER _{hp}	A	PTSA	P	Twarm_well_in	P		
η_{reg}	P			Pboiler	A				

As can be seen, nine symptoms were automatically detected as present and 22 as absent.

8. Evaluation of the results of the automated symptom detection process

For the analysis of the results on an annual basis, the 16-minute and daily data from the BMS were analysed using energy signature graphs for the whole year 2013, which are presented in Appendix B. Below we discuss the results from some of these energy signature graphs. In addition, interviews were conducted with the building manager and log books were consulted which did not lead to additional symptoms.

8.1 Evaluation of energy balance symptoms

In addition to the annual efficiencies as shown in Fig. A.1, the daily efficiencies of systems B, C, D, G and H are estimated (see Fig. B.1). Most deviations remain under the set thresholds, which supports the reliability of the annual detection results for the energy balance symptoms.

8.2 Evaluation of EP symptoms

8.2.1 Performance factors

The daily COP and EER values of the heat pump fluctuate realistically (see Fig. B.2) around the set thresholds with some outliers. The main causes of these outliers are transient behaviour and the fact that the actual COPs and EERs depend on varying water temperatures.

The SEER_{cw} (60) (see Table A.2) was much higher than expected. Additional analysis of the energy data showed that cold was only provided by the cold well of the ATEs system, whereas it was expected during design that the heat pump would deliver 10% of the cold, yielding a lower SEER_{cw} of 40.

8.2.2 Capacities

As for the capacities, 16-minute capacities were checked for the whole the year using graphs and symptoms were not missed. The inadequate capacity of the heat exchanger of the ATES system (PTSA) was correctly diagnosed (see Fig. B.3, which shows the 16-minute graph): the actual capacity remains far below the design value (840 kW) throughout the year.

8.3 Evaluation of OS symptoms

Visual inspection of the energy signatures for the control-based and design-based operational states (see Figs. B.4 to B.16) shows that they are close to the set point where symptoms are absent.

9. Detection time span

The detection process is described in Section 7 for a period of one year. However, where a symptom was found, it is quite clear, as the graphs in Appendix B show, that daily, weekly or monthly analysis could have enabled the symptoms to be found earlier.

Conversely, a short period-level analysis can lead to the identification of a symptom that ultimately rarely occurs (for example, 3.1% of the days in Fig. B.7). It is conceivable that the BEMS would simply warn that there is a potential fault and would only report a real problem after successive days, e.g. by using moving average methods, taking previous results into account to exclude temporary sensor outliers and effects of transient behaviour. This section discusses the use of shorter detection periods. We present results from monthly and daily symptom detection using rules from Section 7.

9.1 Monthly and daily detection of energy balance symptoms

Monthly detection

Table C.1 shows that outliers are not found for systems B, C, G and H using monthly detection based on Eq. (4.3). However, the boiler system D shows two outliers. We note that the exchanged energy of the boiler system was estimated using soft sensors for the flow rate and the return temperature at the boiler header (shown as (21) in Fig. 5.2), which introduces inaccuracies. The presence of hard sensors could lead to lower deviations.

Daily detection

Daily detection for energy balance symptoms (see Fig. B.1) yields reasonable results. Only five false detection results were found, i.e. five outliers in 1825 detection results (<0.3%).

9.2 Monthly and daily detection of energy performance symptoms

Here we discuss the detection time span for EP symptoms. EP symptom detection is more complicated in monthly and daily detection due to the effects of operational conditions.

9.2.1 Performance factors

First, we address performance factors. As an example we discuss the COP of the heat pump because this is one of the most important KPIs of the thermal energy plant. As this COP is strongly dependent on outdoor temperature levels, it is not acceptable to use the annual expected value, such as SCOP_{hp}=4 in Table A.2 (see Fig. B.2), which shows many outliers. The effects of the water temperatures at the heat pump's evaporator and condenser, which are highly dependent on outdoor temperatures, must be considered. The thermodynamic efficiency η_{td} for several conditions could be estimated using the documentation on the heat pump installed. In the range of operational water temperatures in the case study they are between 0.37 and 0.39. Multiplying an assumed value of 0.38 by the COP of the Carnot process yields the expected performance COP_{exp}:

$$COP_{exp} = \eta_{td} \cdot COP_{Carnot} = \eta_{td} \cdot \frac{T_{high}}{T_{high} - T_{low}} \quad (9.1)$$

where:

T_{high} =T_{cond_out} and T_{low} =T_{evap_out} at which η_{td} is calculated.

Monthly detection

As can be seen from Table C.2, from June to August symptoms for the heat pump were incorrectly detected as present. However, in those months the heat pump was off most of the time. Transient behaviour strongly affected the results. To neglect this effect, we propose ignoring detection results from months in which a component is off most of the time.

Daily detection

Fig. 9.1 shows a part of the daily COP of the heat pump and the expected values, taking thresholds of 5% into account. Here again the upper and lower limits are calculated based on Eq. (9.2) for the thresholds. The measured values are showed in blue.

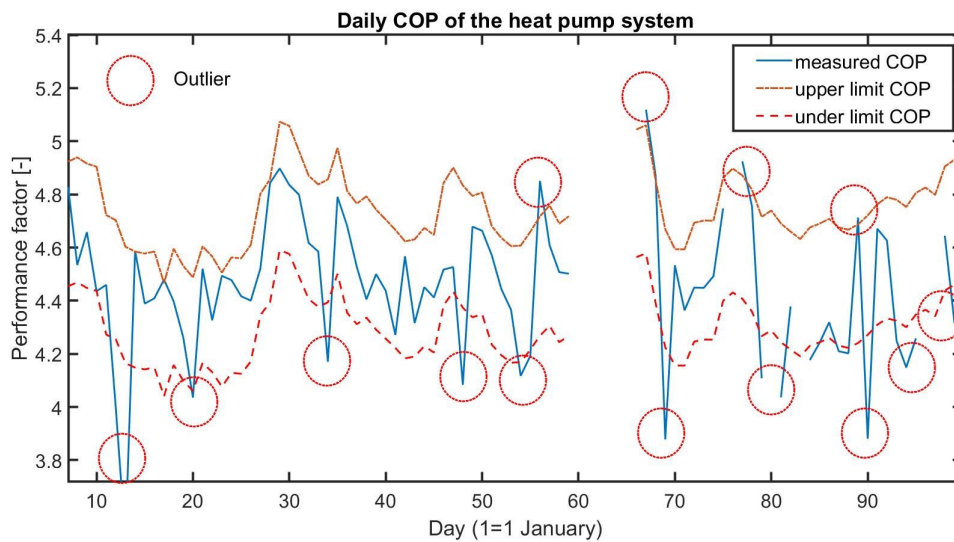


Fig. 9.1 Daily COP of the heat pump system

As can be seen, the actual daily COP follows the expected COP. The heat pump was on for 165 days, with the upper limit exceeded by 21 days and the lower limit by 37 days, caused by transient behaviour and variation in the heat pumps' thermodynamic efficiency η_{td} .

9.2.2 Capacities

We take the boiler capacity as an example to show the monthly maximum heat flux in the gas boiler. There is no point in detecting capacity symptoms on a daily basis, because the nominal capacity is only achieved under full load conditions, which are not present every day. However, Table C.3 shows for example that the boiler capacity can be detected correctly for the winter months, when there is significant heat consumption by the boiler.

9.3 Monthly and daily detection of operational state symptoms

Monthly detection

The number of hours is considered in monthly detection, as opposed to the number of days in annual detection. Only hours that meet the additional condition that the system is on for 30 minutes are considered. Table C.4 shows for example results for Tcond_out, Tcw_supply and Tcold_well_in. False detections are highlighted in yellow.

Tcold_well_in shows no false detection results. However, Tcond_out and Tcw_supply are incorrectly detected as present or absent in some months, which may be due to assumed thresholds that are too low and transient behaviour.

Daily detection

Daily detection of operational state symptoms based on Eq. (4.7) makes no sense because we know from Fig. B.4 to B.14 that this yields many wrong detections.

9.4 Conclusions and recommendations for daily and monthly detection time spans

Overall, we note that daily detection of energy efficiencies yields acceptable detection results. The outliers for the boiler system efficiencies show the need to avoid complex soft sensors as much as possible. In the case of new HVAC systems, the necessary measuring points must be present to avoid complex models for estimating exchanged energy quantities.

Research into additional conditions as mentioned in 4.2.4 is needed: for instance, to take into account hours in which the exchanged energy is higher than a certain threshold. This would avoid incorrect monthly detections of the COP of the heat pump and the boiler capacity, as shown in Appendix C. However, it would also be possible to start up the energy plant, e.g. daily, weekly or monthly, at different full load modes to estimate symptoms earlier.

To increase the reliability of the detection results, especially when using daily detection, we propose researching the use of smoothing techniques which calculate the average deviation based on two or more days, to compensate for daily outliers. In addition to a CUSUM (cumulative sum control chart), one could apply the EWMA (exponentially weighted moving average) chart method (see [28] for implementation).

We also recommend researching the application of this to daily binary detection outcomes (e.g. -1: too low, 0: correct, 1: too high).

Daily detection of the capacities of thermal energy systems makes no sense because full load does not occur every day and start-up every day requires a great deal of energy in full-load mode. However, this is a realistic solution for distribution systems (pump, fans and valves).

Another approach which is applicable to all KPIs is to give a warning that could not lead to direct action on the part of the technical manager or to an automated fault diagnosis.

Diagnosis could take place after structural false detections.

10. Conclusion and recommendations

Current symptom detection methods for energy diagnosis in HVAC systems are not standardised and there is still no classification of detection models with generic key performance indicators and associated detection rules. This paper presents a classification of symptoms into three categories: balance, energy performance and operational states, that covers a large part of encountered symptoms.. Detection models and KPIs are developed for these 3 categories. Generic detection rules for energy diagnosis in heating, ventilation and air conditioning (HVAC) systems are proposed which are consistent with HVAC process and instrumentation diagrams (P&IDs) as used by engineers to design and operate these systems. It has been applied successfully to the thermal energy plant of the THUAS school building. One whole year was taken as the detection period. However, monthly and daily detection also yielded adequate results. Section 10.1 summarises the results for the detection framework in more detail and Section 10.2 draws conclusions from the case study. Section 10.3 proposes recommendations for the standardisation of symptom detection.

10.1 Results of the detection framework based on the 4S3F method

The proposed framework for energy performance analysis falls into four phases: pre-processing, detection, diagnosis and correction. This article focuses on the symptom detection phase based on the 4S3F architecture, which contains four types of symptoms and three types of faults. The three main types of symptoms are discussed, and rules and thresholds are developed:

- Balance symptoms: efficiencies.

- Energy performance (EP) symptoms: performance factors such as COPs and EERs, capacities such as nominal heat and cold rates and flow rates, and energy outliers such as unexpected energy consumption.
- Operational state (OS) symptoms: control-based symptoms such as controlled supply temperatures, and design-based symptoms such as expected return temperatures from energy users.

The approach discussed is congruent with the way engineers design an HVAC system.

The HVAC designer uses the P&IDs for detection purposes. In the pre-processing phase, systems and aggregated systems are determined once by the HVAC designer. For the detection process, the same HVAC designer must list all the possible symptoms (balance, EP and OS based) once that could be occurring in the system based on the measurement points in the P&ID. Each of the symptoms relates to the equations and models described in the present paper, which could easily be compiled into a standard guideline.

The detection process can be fully automated by using generic detection models for aggregated systems such as generator, hydronic and emitter systems. These equations have to be programmed in the BEMS once, preferably producing symptoms at day, week, month, season and annual level.

The next step is to use these symptoms to identify the faults causing them, using the 4S3F methods and DBNs: this will be discussed in detail in another paper. However, the simple fact of having an automated symptom detection system covering a wide range of parameters is already very helpful for energy performance diagnosis.

10.2 Conclusions from the case study

The case study successfully demonstrated the symptom detection part of the 4S3F framework for a thermal energy plant with an ATES system. One whole year, with 16-minute time interval, historical data was examined to show how symptoms leading to faults can be detected automatically.

The evaluation has shown that no symptoms were overlooked or incorrectly detected. Section 9 discussed time spans shorter than one year, showing that the proposed symptom detection method can be used for daily and monthly detection, provided that the recommendations in Section 9.4 are followed.

In our case study, an HVAC commissioning engineer would focus on the nine symptoms detected to optimise the system. In a subsequent paper, we will show that by redesigning the control rules a 25% annual primary energy saving could be achieved in the case study, which is a thermal heat plant with a reputation for working well. This indicates that far more energy savings would be possible if such symptom detection methods were used more widely.

10.3 Recommendations for further research

Although the results are promising, further research is needed. We have not considered developing the fault identification model with a DBN included in the 4S3F framework here.

Further research is needed into the question of which threshold values should be used for the KPIs and that of which symptom detection period (hourly, daily or seasonal) is needed for which systems and subsystems. Given the question of KPI thresholds, research into dynamic KPIs for hourly and daily detection is recommended. It also needs

to be examined whether the HVAC can be started up automatically daily, weekly or monthly by the BMS in different HVAC modes to hasten the detection of symptoms. In addition, a guideline on the minimum BMS dataset needed to estimate energy amounts to and from systems would be helpful. It could be worthwhile to expand the list of symptoms: for instance, with OS symptoms concerning flow rates, valves and pumps. Additional symptoms from maintenance logbooks and commissioning reports were not taken into account but could offer additional possibilities. For automation purposes, a generic library of symptom detection models is needed from which EP models can be selected in a specific case. A start has been made in this paper.

Appendix A Threshold values and results from annual detection

This appendix presents information on threshold values for the four types of symptoms in the 4S3F method in tables. Detection results from annual detection are also presented.

As shown in Table A.1, a symptom is present (depicted as **P**) for η_{reg} . The other symptoms are absent (**A**).

Table A.1 Annual detection results: energy balance symptoms

(**A**: symptom absent; **P**: symptom present)

System	Efficiency	Efficiency in accordance with guideline ISSO 39 [27] or design	Measured efficiency	Symptom detection
ATES system (B)	η_{systB}	0.93	0.94	A
Heat pump system (C)	η_{systC}	0.95	0.95	A
Boiler system (D)	η_{systD}	0.95	0.95	A
Hydronic cold water system (G)	η_{systG}	0.95	0.99	A
Hydronic cold water system (H)	η_{systH}	0.95	0.98	A
ATES system (B)	η_{TSA}	87%	97%	A
ATES system (B)	η_{reg}	1	0.63	P

Table A.2 presents the results for the energy performance factors (EPFs).

Table A.2 Measured annual EPFs and reference annual EPFs

(**A**: indicates symptom absent; **P**: symptom present)

System	EP factor	EP factor in accordance with guideline ISSO 39 [27] or design	Measured SPF	Symptom detected
Whole system (B to D, and H and G)	SCOP _{hw}	3	3	A
Whole system	SEER _{cw}	40	60	A

(B to D, and H and G)				
ATES system (B)	SCOPreg	20	22.3	A
Heat pump system (C)	SCOPhp	4	4.5	A
Heat pump system (C)	SEERhp	3.2	3.6	A
Roof system (F)	SCOProof	20	16.7	P
Hot water capacity (E)	Phw	597	540	A
Cold water capacity (A)	Pcw	742	450	P
Roof collector capacity (F)	Proof	576 kW	531 kW	A
Heat pump capacity (C)	Php	247 kW	270 kW	A
Gas boiler capacity (D)	Pboiler	327 kW	400 kW	A
Capacity of heat exchanger TSA from ATES system (8)	PTSA	840 kW	590 kW	P
Heat regeneration capacity of ATES system (B)	Preg	237 kW	250 kW	A

Tables A.3 and A.4 present results for operational state symptoms. As can be seen, five operational state symptoms were detected.

Table A.3 Thresholds for set-point values and symptoms of control-based indicators

(A: symptom absent P: symptom present)

	Controlled value	Measured by sensor (see Fig. 3.6)	Thresholds	Symptom detected	
Hot water supply (E) (Thw_supply, Fig. 5.2.)	Winter mode: varying linearly between 45 and 35°C at outdoor temperatures between -10 and 15°C. Summer mode: 30°C	TT28-02	$\epsilon_{\max}=3\text{ K}$	$\delta\text{ [%]}$	
			$\delta_{LL}=10\%$	11.1	P
			$\delta_{UL}=10\%$	0.9	A

Cold water supply (A) (T _{cw_supply} , Fig. 5.3.)	Varying linearly between 15 to 11°C at outdoor temperatures between 15 and 25°C	TT29-02	$\epsilon_{\max} = 1 \text{ K}$	δ [%]	
			$\delta_{LL}=10\%$	0.5	A
			$\delta_{UL}=10\%$	22.8	P
Outlet of cold water heat pump (C) (T _{cond_out} , Fig. 5.4)	8.5°C in winter mode	TT04-01	$\epsilon_{\max} = 3 \text{ K}$	δ [%]	
			$\delta_{LL}=10\%$	3.1	A
			$\delta_{UL}=10\%$	4.0	A
Outlet of evaporator (C) (T _{evap_out} , Fig. 5.5)	7°C in winter mode	TT04-04	$\epsilon_{\max} = 1 \text{ K}$	δ [%]	
			$\delta_{LL}=10\%$	0.9	A
			$\delta_{UP}=10\%$	3.1	A
Inlet of cold water well (B) (T _{cold_well_in} , Fig. 5.6)	7.5°C	TT02-01	$\epsilon_{\max} = 1 \text{ K}$	δ [%]	
			$\delta_{LL}=10\%$	0.0	P
			$\delta_{UL}=10\%$	68.5	A
Inlet of warm water well (B) (T _{warm_well_in} , Fig. 5.7)	17.5°C, 20°C in regeneration mode	TT02-03	$\epsilon_{\max} = 1 \text{ K}$	δ [%]	
			$\delta_{LL}=10\%$	18.9	P
			$\delta_{UL}=10\%$	8.3	A

Table A.4 Thresholds for design-based indicators and symptom detection

(**A**: symptom absent **P**: symptom present)

	Design value	Measured by sensor (see Fig. 3.6)	Thresholds	No symptom detected	
				δ [%]	
Hot water return (E) (T _{hw_return} , Fig. 5.8)	35°C in winter mode, 24°C in summer mode	TT28-03	$\epsilon_{\max} = 3 \text{ K}$ $\delta_{UL}=10\%$	69.9	A
Cold water return (A) (T _{cw_return} , Fig. 5.9)	19°C	TT29-04	$\epsilon_{\max} = 1 \text{ K}$ $\delta_{LL}=10\%$	9.2	A
Input of evaporator (C) (T _{evap_in} Fig. 5.10)	12°C in winter mode, 19°C in summer mode	TT04-05	$\epsilon_{\max} = 1 \text{ K}$ $\delta_{UL}=10\%$	0.0	A
Outlet of cold water well (B) (T _{cold_well_out} , Fig. 5.11)	8.5°C in summer mode	TT02-01	$\epsilon_{\max} = 1 \text{ K}$ $\delta_{UL}=10\%$	7.8	A
Outlet of warm water well (B) (T _{warm_well_out} , Fig. 5.12)	16.5°C in winter mode	TT02-03	$\epsilon_{\max} = 1 \text{ K}$ $\delta_{LL}=10\%$	48.7	P

Appendix B Results from daily detection

his appendix presents results from daily detection. Fig. B.1 shows the daily deviations of the systems B to D, G and H. As can be seen, they almost all remain under the threshold of 5%.

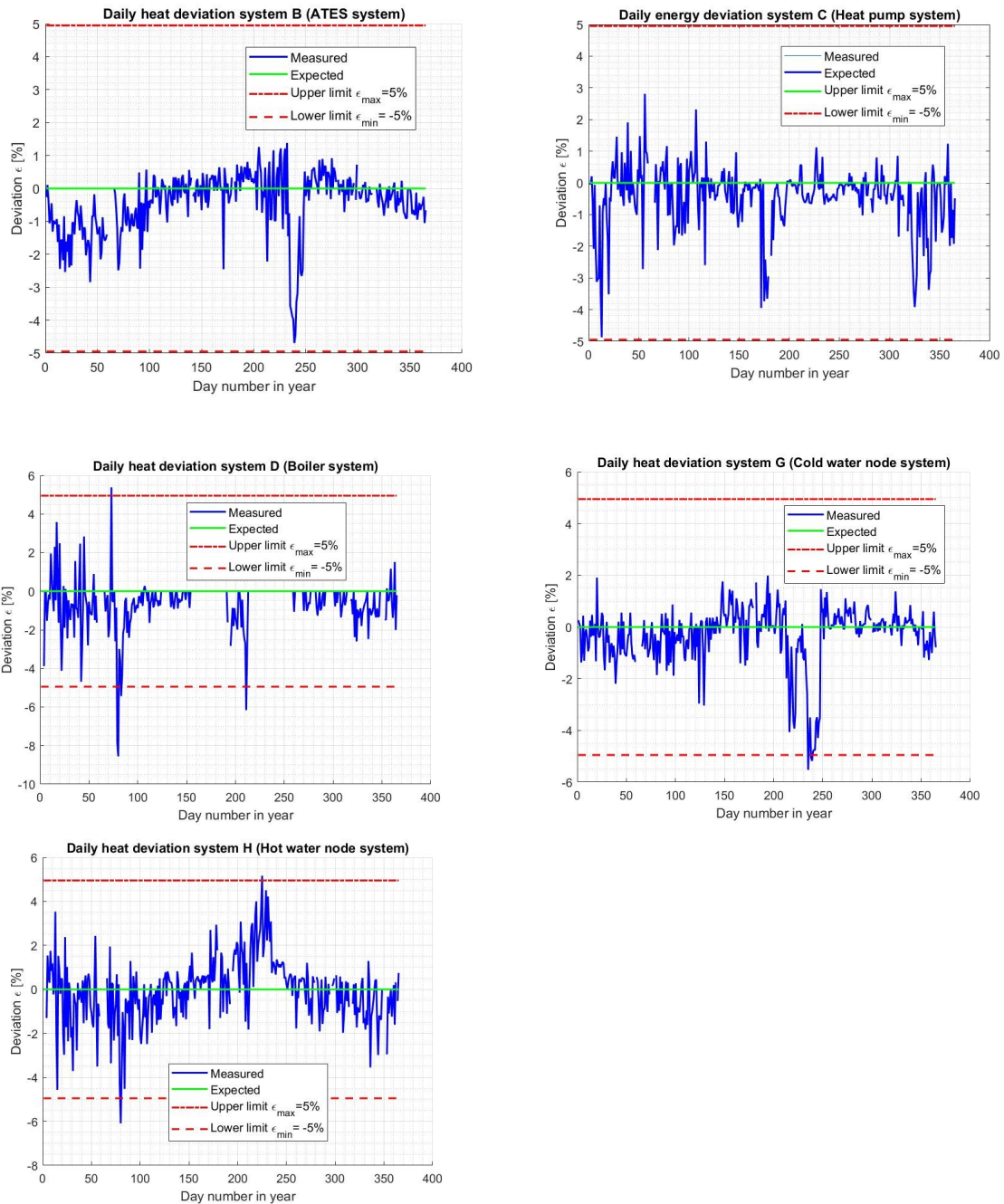


Fig. B.1 Daily efficiencies of systems B, C, D, G and H

Fig. B.2 shows the daily COPs and EERs of the heat pump system.

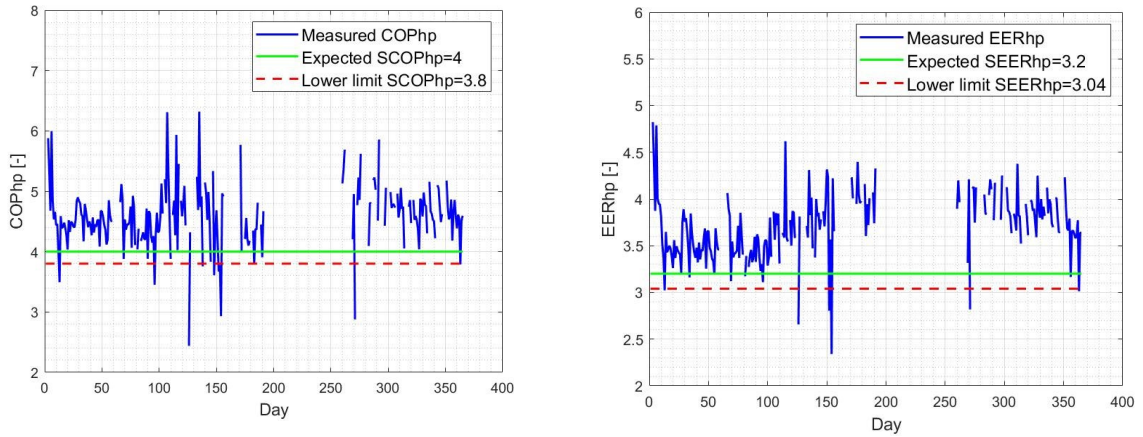


Fig. B.2 Daily energy performance factors of the heat pump

The maximum heat flux of the heat exchanger TSA of the ATES system is shown in Fig. B.3 based on 16-minute time spans. Positive values are present when the warm well is used, negative when the cold well is used.

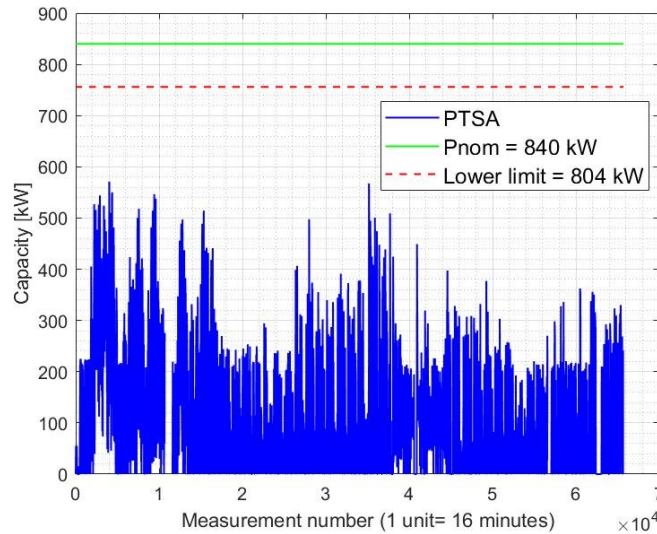


Fig. B.3 Measured capacity of the heat exchanger (TSA) of the ATES system throughout the year 2013 (based on 16-minute measurements)

Figs. B.4 to B.14 show energy signatures for operational states. One year was taken as the detection period. Each point indicates the result of one day. A detected symptom is indicated as **P** and as **A** when absent. n_{tot} represents the number of days for which the system that affects the operational state is active.

As a reference, each figure shows the values expected from the control set points or the design values. The acceptable limits ϵ_{min} and ϵ_{max} for ΔT are shown as presented in Tables A.3 and A.4. In these graphs ‘no symptom detected’ is indicated by an **A** (absent) and ‘a symptom detected’ by a **P** (present), in line with Tables A.3 and A.4. A value in brackets indicates that a threshold was not set.

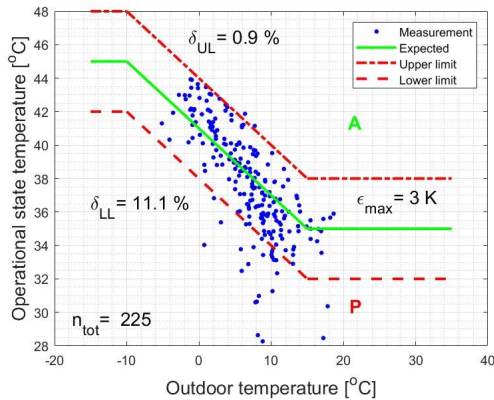


Fig. B.4 Energy signature of Thw_supply

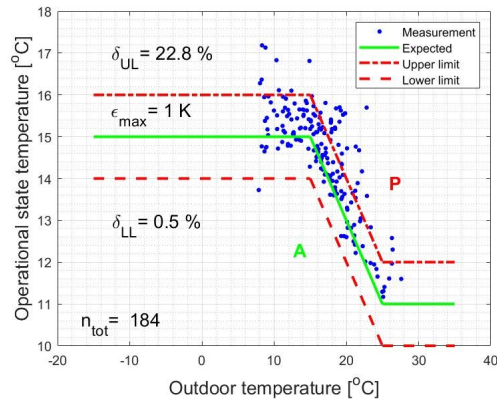


Fig. B.5 Energy signature of Tcw_supply

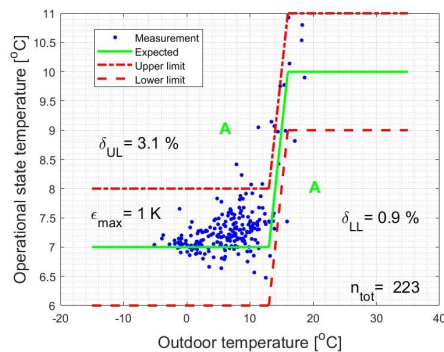
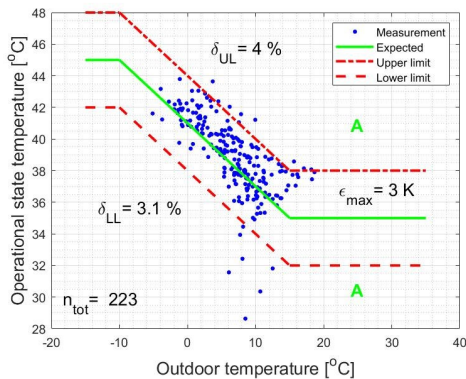


Fig. B.6 Energy signature of Tcond_out

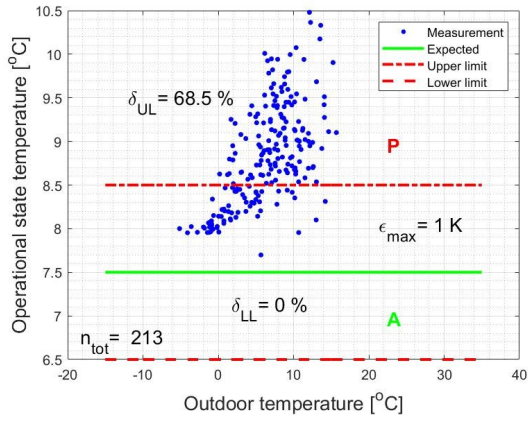


Fig. B.7 Energy signature of Tevap_out

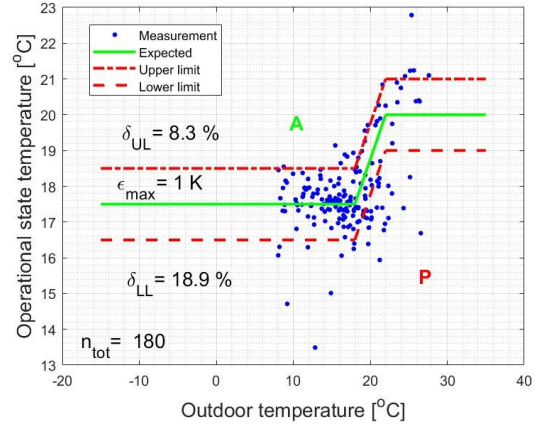


Fig. B.8 Energy signature of Tcold_well_in

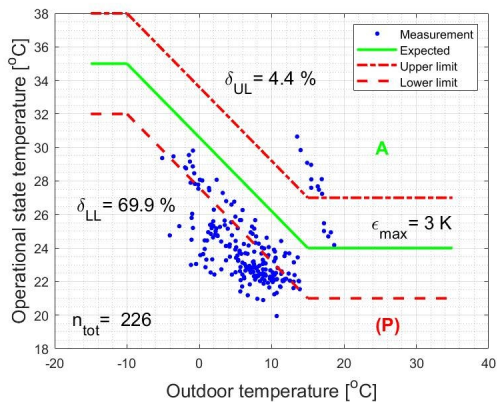


Fig. B.9 Energy signature of Twarm_well_in

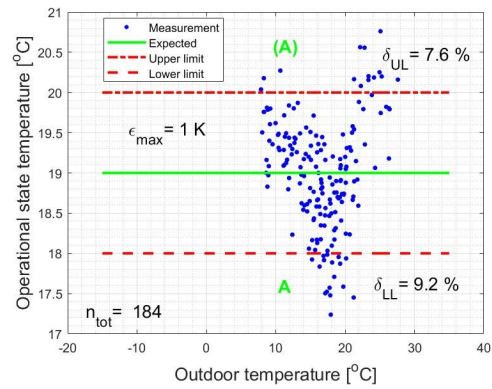


Fig. B.10 Energy signature of Thw_return

Fig. B.11 Energy signature of Tcw_return

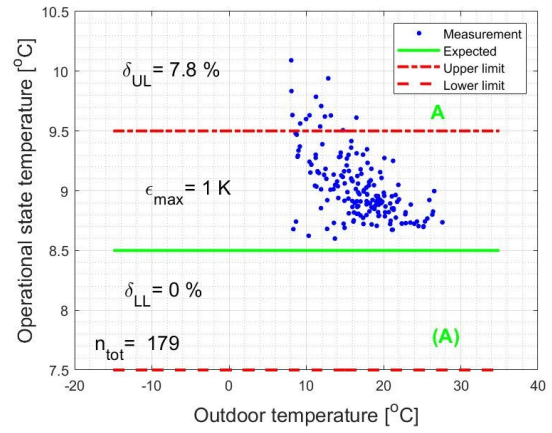
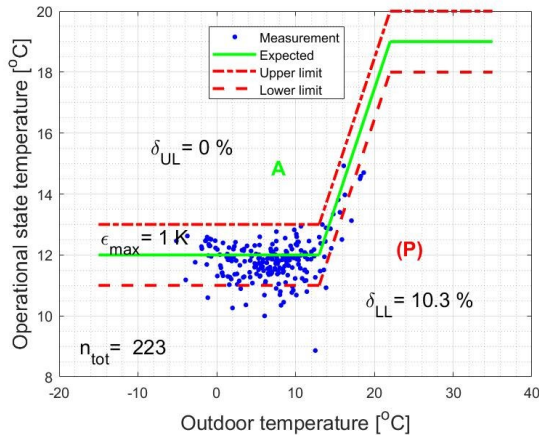


Fig. B.12 Energy signature of T_{evap_in}

Fig. B.13 Energy signature of $T_{cold_well_out}$

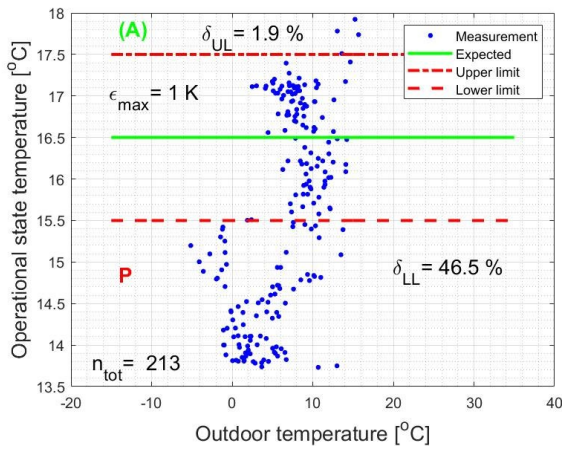


Fig. B.14 Energy signature of $T_{warm_well_out}$

Appendix C Results from monthly detection

This appendix presents some detection results from monthly detection periods. False detection results, deviating from the annual outcomes, are shown highlighted in yellow.

Table C.1 shows the outcomes for the boiler system D.

Table C.1 Monthly energy balance symptoms of boiler system D
(yellow: incorrect detection)

Yellow: Symptom is present (δ_{UL} =above upper limit, δ_{LL} =under lower limit, NA=not available, n_{day} =number of operational days)

Symptom	Jan	Feb	Mar	Apr	May	Jun	Jul	Aug	Sep	Oct	Nov	Dec	Annual
ε [%]	-2	-3	-7	-3	-1	0	-5	0	-1	-2	-3	-3	-0.4
Qboiler_mod [GJ]	60	35	66	12	3	0	3	0	0	0	1	13	198

Table C.2 shows the monthly deviation ε of the SCOP of the heat pump based on the days in the month n_{days} for which the SCOP could be estimated. The heat produced monthly is divided by the work supplied by the heat pump monthly to estimate the measured monthly SCOP_{hp}. The reference SCOP_{exp} is calculated using Eq. (9.1). As can be seen from this table, a monthly detection period leads to symptoms for June to September despite the fact that the annual SCOP for the heat pump apparently indicates a correct COP.

Table C.2 Monthly SCOP symptoms of the heat pump on a daily basis
(yellow: incorrect detection)

Yellow: Symptom is present, ε =deviation between SCOP_{hp} and SCOP_{exp}

Symptom	Jan	Feb	Mar	Apr	May	Jun	Jul	Aug	Sep	Oct	Nov	Dec	Annual
SCOP _{hp}	4.5	4.5	4.4	4.5	4.7	4.2	3.9	0.0	4.9	4.9	4.7	4.7	4.5
SCOP _{exp}	4.5	4.5	4.5	4.7	4.8	5.0	5.0	5.0	4.9	4.9	4.7	4.7	4
ε [%]	1.1	0.0	-1.2	-3.3	-2.5	-16	-23	-101	-1.3	1.6	-0.9	0.0	12.5
Qcond_mod [GJ]	316	282	166	102	33	21	7	0	8	33	115	192	1313

The maximum heat flux measured in each month is shown in Table C.3. As can be seen, capacity is low in the months May to November.

Table C.3 Symptoms for the capacity of the boiler (yellow: false detection)

Symptom	Jan	Feb	Mar	Apr	May	Jun	Jul	Aug	Sep	Oct	Nov	Dec	Annual
Pboiler	T	T	T	T	F	F	F	-	F	F	F	T	T
Pmax [kW]	394	380	400	311	227	67	22	NaN	56	63	62	377	400

Table C.4 presents the results for monthly symptoms for three OS variables considered in the case study: Tcond_out, Tcw_supply and Tcold_well_in. In this table δ_L and δ_H represent the monthly percentage by which the lower and upper limit thresholds are exceeded, calculated using Eq. (4.8). Those hours n_{tot} are shown in Table B.4 for each month. For those hours an exceeded threshold is added to n_{fault} as a counter. This table also shows the exchanged energy E_{month} during those hours.

Table C.4 Monthly OS symptoms (yellow: incorrect detection)

(δ_{UP} =above upper limit, δ_{LL} =under lower limit, NA=not available, n_{tot} =number of operational hours or days, E_{month} =exchanged energy)

Symptom		Jan	Feb	Mar	Apr	May	Jun	Jul	Aug	Sep	Oct	Nov	Dec	Annual
Tcond_out	δ_{UL} [%]	0	0	0	11.1	9.1	20.0	75.0	NA	0	0	4	0	4
	δ_{LL} [%]	6.9	0	4.2	3.7	4.5	0	0	NA	16.7	5.9	0	0	3.1
	n_{tot} [hr]	347	316	208	120	33	23	3	0	7	33	155	247	223 days
	E_{month} [GJ]	65	58	36	21	6	4	0	0	1	5	23	38	
Tcw_supply	δ_{UL} [%]	100	NA	0	17.6	4.5	4.2	8.0	20.0	53.3	17.4	0	0	22.8
	δ_{LL} [%]	0	NA	0	0	0	0	0	0	0	0	0	100	0.5
	n_{tot} [hr]	0	0	7	42	96	225	241	256	619	87	6	0	184 days

	E_{month} [GJ]	0	0	3	18	53	157	213	140	297	37	2	0	
Tcold_well_in	δ_{UL} [%]	17.9	10.7	16.0	70.4	94.7	88.9	100	NA	100	76.5	92	61.5	68.5
	δ_{LL} [%]	0	0	0	0	0	0	0	NA	0	0	0	0	0
	n_{tot} [hr]	398	370	291	140	32	16	2	0	6	32	174	265	213 days
	E_{month} [GJ]	441	346	229	76	8	2	0	0	1	10	81	181	

References

- [1] P. de Wilde, The gap between predicted and measured energy performance of buildings: A framework for investigation. *Automation in Construction* 41 (2014) 40-49. <https://doi.org/10.1016/j.autcon.2014.02.009>.
- [2] A. Taal, L. Itard, W. Zeiler, A referenced architecture for the integration of automated energy performance fault diagnosis into HVAC systems, *Energy & Buildings* 179 (2018) 144-155, <https://doi.org/10.1016/j.enbuild.2018.08.031>.
- [3] L. Haorong, Y. Daihong, J., Braun (2011), A review of virtual sensing technology and application in building systems, *HVAC&R Research*, 17:5, 619-645, <https://www.tandfonline.com/doi/abs/10.1080/10789669.2011.573051>. [accessed 30.03.2020]
- [4] BuildingEQ. <http://www.buildup.eu/en/practices/cases/building-eq-tools-and-methods-linking-epbd-and-continuous-commissioning> [accessed 20.06.2019]
- [5] European Standard EN 15316-1:2017. Energy performance of buildings. Method for calculation of system energy requirements and system efficiencies. General and Energy performance expression, Module M3-1, M3-4, M3-9, M8-1, M8-, CEN, Brussels, 2017.
- [6] W. Kim, S. Katipamula. A Review of Fault Detection and Diagnostics Methods for Building Systems. *Science and Technology for the Built Environment*, 24:1, 3-21, <https://doi.org/10.1080/23744731.2017.1318008>.
- [7] Z. Guo, X.Liu, W. Tao, R. Shah. Effectiveness–thermal resistance method for heat exchanger design and analysis. *International Journal of Heat and Mass Transfer* Volume 53, Issues 13–14, June 2010, Pages 2877-2884 <https://doi.org/10.1016/j.ijheatmasstransfer.2010.02.008>

[8] L.Gao, J. Zhao, Q. An, J. Wang, X. Liu. A review on system performance studies of aquifer thermal energy storage. *Energy Procedia* 142 (2017) 3537-3545.

<https://doi.org/10.1016/j.egypro.2017.12.242>

[9] W. Chung. Review of building energy-use performance benchmarking methodologies. *Applied Energy* 88 (2011) 1470-1479.

<https://doi.org/10.1016/j.apenergy.2010.11.022>.

[10] J. Liu, H. Chen, J. Liu, Z. Li, R. Huang, L. Xing. An Energy performance evaluation methodology for individual office building with dynamic energy benchmarks using limited information. *Applied Energy* 206 (2017) 193-205.

<https://doi.org/10.1016/j.apenergy.2017.08.153>

[11] Y. Wei, X. Zhang, Y. Shi, L. Xia, S. Pan, J. Wu, M. Han. A review of data-driven approaches for prediction and classification of building energy consumption. *Renewable and Sustainable Energy Reviews* 82 (2018) 1027-1047.

<https://doi.org/10.1016/j.rser.2017.09.108>.

[12] E.H. Borgstein, R. Lamberts, J.L.M. Hensen. Evaluating energy performance in non-domestic buildings: A review. *Energy and Buildings* 128 (2016) 734-755.

<https://doi.org/10.1016/j.enbuild.2016.07.018>.

[13] Z. Li, Y. Han, P.Xu. Methods for benchmarking building energy consumption against its past or intended performance: An review. *Applied Energy* 124 (2014) 325-334. <https://doi.org/10.1016/j.apenergy.2014.03.020>.

[14] H. Wang, P. Xu, X. Lu, D. Yuan. Methodology of comprehensive building energy performance diagnosis for large commercial buildings at multiple levels. *Applied Energy* 169 (2016) 14-27. <https://doi.org/10.1016/j.apenergy.2016.01.054>.

- [15] R. Hitchin, I. Knight, Daily energy consumption signatures and control charts for air-conditioned buildings. *Energy and Buildings* 112 (2016) 101-109.
<https://doi.org/10.1016/j.enbuild.2015.11.059>.
- [16] J. Bynum, D. Claridge, J. Curtin, Development and testing of an Automated Building Commissioning Analysis Tool (ABCAT). *Energy and Buildings* 55 (2012) 607-617. <https://doi.org/10.1016/j.enbuild.2012.08.038>.
- [17] G. Anzaldi, A. Corchero, H. Wicaksono, K. McGlenn, A. Gerdelan, M. Dibley. Knoholem: Knowledge-Based Energy Management for Public Buildings Through Holistic Information Modeling and 3D Visualization. https://doi.org/10.1007/978-3-319-02332-8_5.
- [18] T. Maile, V. Bazjanac, M. Fisher. A method to compare simulated and measured data to assess building energy performance. *Building and Environment* 56 (2012) 241-251. <https://doi.org/10.1016/j.buildenv.2012.03.012>.
- [19] D. Choiniere, D. DABOTM: A BEMS assisted on-going commissioning tool. *Proceedings of the National Conference on Building Commissioning*. 2008.
<https://www.bcx.org/ncbc/2008/docs/Choiniere.pdf>
- [20] L. Belussi, L. Danza. Method for the prediction of malfunctions of buildings through real energy consumption analysis: Holistic and multidisciplinary approach of Energy Signature. *Energy and Buildings* 55 (2012) 715-720.
<https://doi.org/10.1016/j.enbuild.2012.09.003>.
- [21] A. Costa, M. Keane, J. Torrens, E. Corry. Building operation and energy performance: Monitoring, analysis and optimization toolkit. *Applied Energy* 101 (2013), 310-306. (WBD). <https://doi.org/10.1016/j.apenergy.2011.10.037>.

[22] L. Zhao, J. Zhang, R. Liang. Development of an energy monitoring system for large public buildings. *Energy and Buildings* 66 (2013) 41-48.

<https://doi.org/10.1016/j.enbuild.2013.07.007>.

[23] A. Ahmed, J. Ploennig, K. Menzel, B. Cahill, Multi-dimensional building performance data management for continuous commissioning, *Advanced Engineering Informatics* 24 (2010) 466-475. <http://dx.doi.org/10.1016/j.aei.2010.06.007>

[24] J. Liu, H. Chen, J. Liu, Z. Li, R. Huang, L. Xing, J. Wang, G. Li, An energy performance evaluation methodology for individual office building with dynamic energy benchmarks using limited information. *Applied Energy* 206 (2017) 193-205.

<https://doi.org/10.1016/j.apenergy.2017.08.153>

[25] C. Miller, Z. Nagy, A. Schlueter. Automated daily pattern filtering of measured building performance data. *Automation in Construction* 49 (2015) 1-17.

<https://doi.org/10.1016/j.autcon.2014.09.004>

[26] B. Bozkaya, R. Li, W. Zeiler. A dynamic building and aquifer co-simulation method for thermal imbalance investigation. *Applied Thermal Engineering* 144 (2018) 681-694.

<https://doi.org/10.1016/j.applthermaleng.2018.08.095>.

[27] ISSO-publicatie 39, Energiecentrale met warmte en koude opslag (WKO). ISSO. 2017. ISBN: 978-90-5044-307-4978-90-5044-307-4.

[28] Y. Zhao, S. Wang, F. Xiao, A system-level incipient fault-detection method for HVAC systems. *HVAC&R Research*, 19:5, 593-601. <http://hdl.handle.net/10397/23739>